Published online 4 June 2012 *Nucleic Acids Research, 2012, Vol. 40, No. 16* ***7975–7984***
doi:10.1093/nar/gks523

Single-molecule microscopy reveals new insights into nucleotide selection by DNA polymerase I

Radoslaw P. Markiewicz, Kyle B. Vrtis, David Rueda* and Louis J. Romano*

Department of Chemistry, Wayne State University, Detroit, MI, USA

Received April 5, 2012; Revised May 9, 2012; Accepted May 10, 2012

ABSTRACT

The mechanism by which DNA polymerases achieve their extraordinary accuracy has been intensely studied because of the linkage between this process and mutagenesis and carcinogenesis. Here, we have used single-molecule fluorescence microscopy to study the process of nucleotide selection and exonuclease action. Our results show that the binding of *Escherichia coli* DNA polymerase I (Klenow fragment) to a primer-template is stabilized by the presence of the next correct dNTP, even in the presence of a large excess of the other dNTPs and rNTPs. These results are consistent with a model where nucleotide selection occurs in the open complex prior to the formation of a closed ternary complex. Our assay can also distinguish between primer binding to the polymerase or exonuclease domain and, contrary to ensemble-averaged studies, we find that stable exonuclease binding only occurs with a mismatched primer terminus.

INTRODUCTION

The incorporation of a nucleotide by a DNA polymerase is an extraordinarily accurate process that is repeatedly required for the faithful duplication of the genome prior to cell division. Although this single catalytic step has been thoroughly studied for over five decades, it is still not completely understood and continues to be the subject of a great deal of interest. *Escherichia coli* DNA polymerase I, first discovered in 1956 (1), has served as a model for the elucidation of this catalytic mechanism and it remains one of the most intensively studied polymerases. Proteolysis of DNA polymerase I produces the Klenow fragment (KF) which contains the polymerase and the 3′–5′ exonuclease (proofreading) domains (2,3). Numerous DNA polymerase crystal structures have shown that many of the structural features first observed for KF are present in high-fidelity polymerases isolated from a variety of sources (4). It is therefore not surprising that these polymerases also share many mechanistic features.

The first step in the catalytic cycle is the association of the polymerase with the primer-template complex (Figure 1a). This is the only step not repeated during processive DNA synthesis. Once bound, the polymerase must select the dNTP complementary to the templating base from a pool of four dNTPs and four rNTPs and this step provides most of the accuracy observed in this synthetic process. For high-fidelity polymerases, it is well established that, once the correct dNTP base pairs with the templating base in the polymerase active site, catalysis involves a nucleotide-induced conformational change of the so called fingers region of the polymerase (5). Recent single-molecule studies have shown that the unliganded polymerase molecule undergoes rapid conformational dynamics between the open and closed form, while for the ternary KF–DNA–dNTP complex the closed conformation dominates (6). This conformational change results in the formation of a tight binding pocket around the nascent base pair that aligns the 3′-OH of the primer with the α-phosphate of the dNTP allowing phosphodiester bond formation to proceed (7–12). On the rare occasion in which KF incorporates a mismatched nucleotide, it has been proposed that the terminal base pairs melt, transferring the primer strand to the exonuclease site located ∼35 Å away from the polymerization site and allowing the proofreading activity to excise the incorrect nucleotide (13). Several studies using a correctly paired primer-template have observed significant levels of binding of the primer to the exonuclease site (14–17), while a recent report suggests that this occurs <3% of the time (18).

In this study, we have monitored the formation of the KF–DNA binary complex in real time and measured the response to internal and external factors using single-molecule Förster resonance energy transfer (smFRET)

*To whom correspondence should be addressed. Tel: +313 577 2584; Fax: +313 577 8822; Email: ljr@chem.wayne.edu
Correspondence may also be addressed to David Rueda. Tel: +313 577 6918; Fax: +313 577 8822; Email: david.rueda@wayne.edu

The authors wish it to be known that, in their opinion, the first two authors should be regarded as joint First Authors.

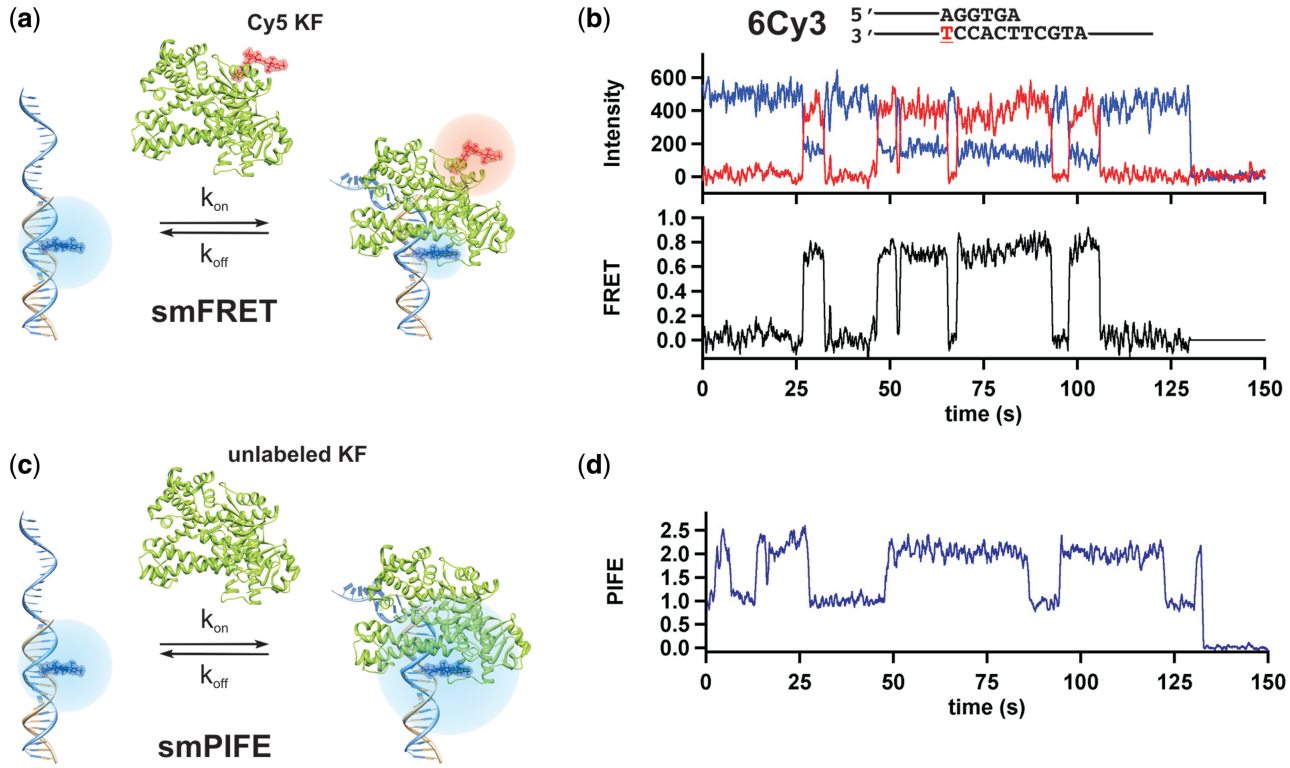

Figure 1. Real time single-molecule measurements of KF binding to DNA. (**a**) Schematic of single-molecule FRET design. Upon KF binding to the primer-template, energy is transferred from the Cy3 (blue) on the DNA template to the Cy5 (red) conjugated to KF (**b**, top). The structure of the primer-template (the 6Cy3 label refers to the fact that there are 6 nt between the Cy3 and the primer terminus) is shown above. Representative donor (blue) and acceptor (red) time trajectories for KF binding to 6Cy3 (**b**, bottom) FRET trace for the trajectory shown in (b, top). Photobleaching of Cy3 occurred at ~130 s. (**c**) Schematic of single-molecule PIFE design. Upon unlabeled KF binding to the primer-template shown in (b, top), the fluorescence intensity of the Cy3 is enhanced ~2-fold. (**d**) Representative PIFE trace for KF binding to 6Cy3. Photobleaching of Cy3 occurred at ~130 s.

and single-molecule protein-induced fluorescence enhancement (smPIFE) (19). By measuring the dynamics for polymerase–DNA binding under a variety of solution conditions, we quantify the stabilizing effect of the next correct nucleotide, as well as, the destabilizing effect of incorrect dNTPs and rNTPs. We find that the polymerase can reject incorrect nucleotides in the presence of the correct dNTP without significantly destabilizing the complex. These results provide further evidence for a mechanism in which nucleotide selection occurs predominantly in the open complex prior to fingers closing and the formation of the tight binding pocket. Finally, we were also able to distinguish between binding of the primer terminus to the polymerase or exonuclease domain and, challenging most ensemble-averaged studies, found that a complementary primer remains bound exclusively to the template at the polymerase active site.

MATERIALS AND METHODS

Klenow fragment purification and labeling

Plasmid pX5106, carrying the KF_{exo-} (D424A) gene and *E. coli* strain CJ376 were generous gifts from Dr C. Joyce (Yale). Enzyme was purified as described (20). Purity exceeded 98% as assessed by SDS–PAGE (data not shown) and ESI–MS (Supplementary Figure S1a and S1b). KF containing a single native cysteine (C907) was incubated in 50 mM Tris–HCl buffer, pH 7.0, 120 μM tris(2-carboxyethyl)phosphine with 5- to 10-fold molar excess of Cy5 maleimide (GE healthcare) for 1 h at room temperature. Reaction was stopped with 10 mM dithiothreitol (DTT). Cy5 labeled enzyme was separated from the free dye on polyacrylamide Bio-Gel P6 spin columns. These stringent reaction conditions yield ~70% KF conjugation to Cy5 and minimize doubly labeled species (Supplementary Figure S1c and S1d). Enzyme activity was measured by primer extension on 20% polyacrylamide gel (Supplementary Figure S2). Cy5 labeling did not affect enzyme activity (21).

DNA oligonucleotide purification and labeling

Primers with 5′-Cy3 or 5′-biotin and amino-modified C6-dT templates were custom synthesized by Eurofins MWG Operon. DNA oligonucleotides were purified by HPLC chromatography on analytical C18 column. Purified oligonucleotides were desalted and their purity was assessed by MALDI-TOF MS. Purified DNA oligonucleotides were homogenous. Exact sequences are shown in Supplementary Table S1. All experiments were performed with the long template unless otherwise stated.

Amino-modified C6-dT 28- and 33-mer templates (Figure 2a) were labeled with Cy3 NHS ester (GE healthcare) using *N*,*N*-diisopropyl-*N*-ethylamine (DIPEA) as the basic agent. Briefly, a reaction containing 10 µl dioxane, 10 µl dimethyl formamide, 3 µl DIPEA and 1 nmol of desalted, amine-modified DNA oligonucleotide was incubated with 10 nmol of the Cy3 NHS ester for 2 h at room temperature. Upon 10-fold dilution with buffer containing 0.1 M triethylammonium acetate pH 7.5, 5% acetonitrile, the reaction mix was directly injected onto a C18 analytical column and the Cy3-modified oligonucleotides were collected (yields ≥90%). Purified oligonucleotides were desalted, characterized by MALDI-TOF MS and stored at −20°C in 10 mM Tris, pH 7.5, 1 mM EDTA buffer.

Dideoxy-terminated primers were synthesized enzymatically by single nucleotide extension reaction catalyzed by deoxynucleotydyl transfarase (TDT). DNA oligonucleotide (1.2 nmol), TDT (45 U) and 100-fold excess of appropriate dideoxy-nucleotide-5′-triphosphate were incubated in the manufacturer's buffer (USB Affymetrix, Inc.) for 6 h at 37°C. Products were purified and analyzed as the Cy3-modified oligonucleotides.

Single-molecule measurements

Quartz slides and cover slips were prepared as described (21–23). DNA was surface-immobilized by washing the slide with streptavidin (0.2 mg/ml) followed by incubation with the biotinylated primer-template duplex (20 pM)

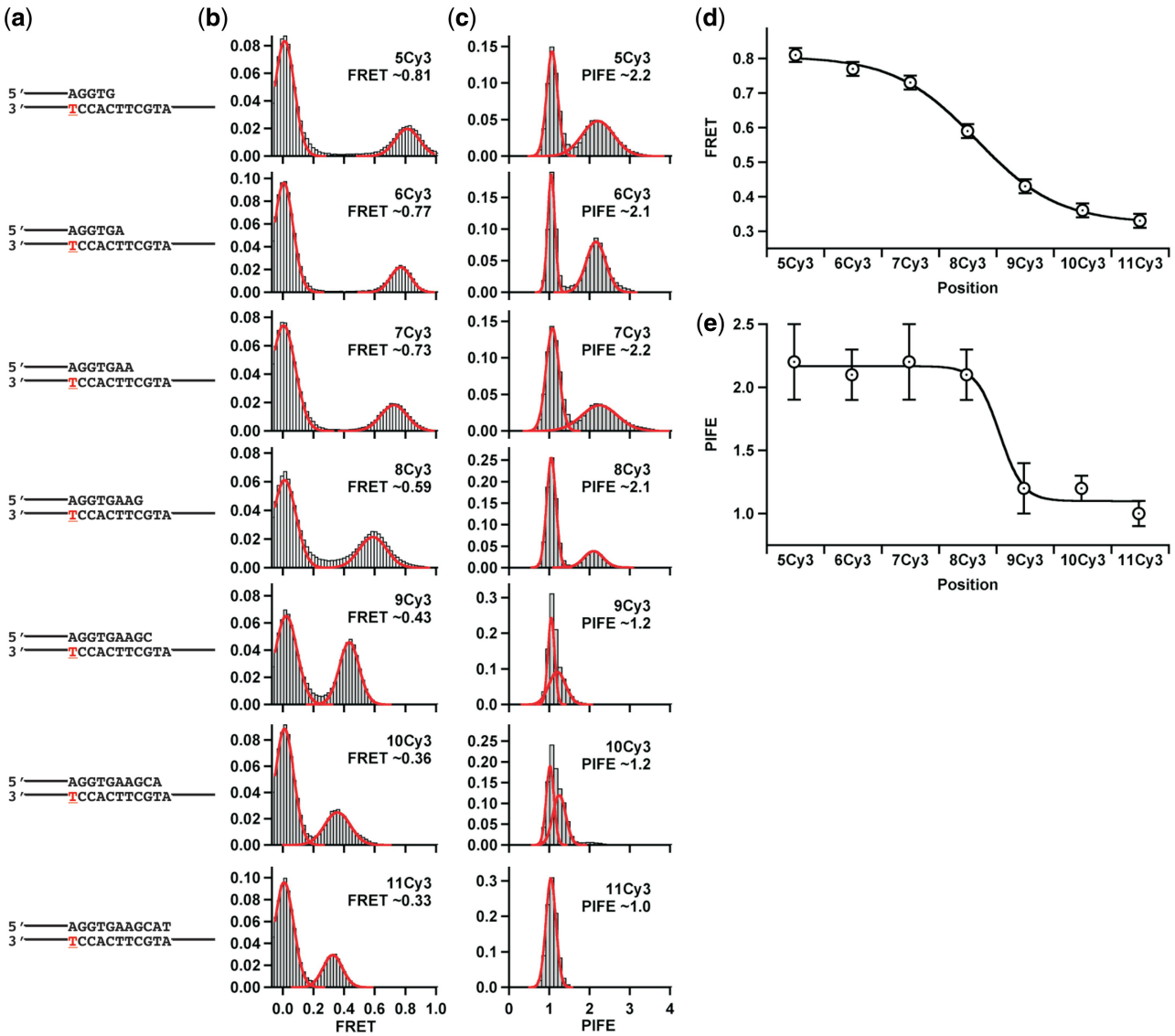

Figure 2. Tracking the position and footprint of KF on the primer-template with smFRET and smPIFE. (**a**) The structure of DNA duplex is shown for each primer-template. The Cy3 is conjugated to the thymine shown in red by an amine linker. (**b**) smFRET efficiency histograms for KF binding to each duplex. (**c**) smPIFE histograms for KF binding to each duplex. (**d**) smFRET efficiencies from (b) were plotted as a function of the distance between the Cy3 and the primer-template terminus. (**e**) PIFE values from (c) were plotted as a function of the distance between the Cy3 and the primer-template terminus. The errors for (d) are estimated to be ±0.02 and the errors for (e) are one-half the width at half maximum amplitude of the peaks. The errors are attributed to the noise of the experiments as opposed to subtle movement of the polymerase on the DNA.

for 8 min. Data was acquired on a home-built, prism-based total internal reflection fluorescence microscope, as previously described (21). Measurements were performed in 50 mM Tris–HCl, pH 7.5, 10 mM Mg, 1 mM DTT, 50 μg/ml BSA and an oxygen scavenging system (4% wt/vol glucose, 0.04 mg/ml glucose oxidase, 0.008 mg/ml catalase). Enzyme concentration and additives are as indicated. The apparent FRET efficiencies were calculated by dividing acceptor intensity (I_A) by the sum of donor and acceptor intensities ($I_D + I_A$). smPIFE and smFRET measurements were performed at ~50 ms time resolution. Experiments in the presence of the next correct dNTP were carried out at ~100 ms time resolution and decreased laser power due to the long binding events. Single-molecule time trajectories were analyzed with either five or seven point moving average. smPIFE and smFRET histograms were created from over 100 single-molecule time trajectories, except for the NaCl titration, which includes at least 50 trajectories per concentration point. Up to 5% of the molecules for any given experiment were excluded from the analysis due to aberrant photophysical or binding behavior. Slightly larger numbers of molecules were excluded for experiments containing the next correct nucleotide.

RESULTS

Tracking KF on a DNA template with base pair resolution

Similar to our prior studies (21), we have used smFRET to observe the dynamics of a Cy5-labeled DNA polymerase (Cy5-KF) on a Cy3-labeled DNA template (Figure 1a). smFRET enables monitoring transient events from individual molecules that are otherwise hidden in ensemble-averaged experiments (21,24,25), therefore revealing KF–DNA binding and dissociation in real time. The nomenclature 'nCy3' indicates the number of base pairs (n) between the Cy3 position on DNA and the primer-template junction (Figure 2a). Control experiments confirm stoichiometric labeling and proper function of the labeled samples (Supplementary Figures S1 and S2).

In the absence of KF, Cy3 emission appears constant and the resulting FRET ratio is zero (Supplementary Figure S3a). In the presence of Cy5-KF, the donor intensity exhibits random decreases accompanied by anti-correlated increases in the acceptor intensity, indicating Cy5-KF binding to 6Cy3 DNA (Figure 1b). The apparent FRET ratio for the binary complex is ~0.77 (Figure 1b). During the experimental time window of ~150 s, several binding events were observed and, within experimental noise, each binding event reached the same FRET ratio.

To track the position of Cy5-KF on the DNA, we used multiple nCy3 constructs with n ranging from 5 to 11 (Figure 2a). For each nCy3 binary complex, the resulting histograms reveal the corresponding FRET ratios ranging from 0.81 for 5Cy3 to 0.33 for 11Cy3 (Figure 2b). No transitions were observed between these different states, indicating that KF binds the primer-template junction in a well-defined orientation. The different FRET ratios obtained for binding to 7Cy3 to 10Cy3 were large enough to allow us to measure binding position with single nucleotide resolution (Figure 2d).

Next, we tested if the observed FRET efficiencies for different binary complexes are independent of the DNA sequence and the length of the DNA primer-template duplex. In these experiments, we used an AT rich template with a shorter duplex region (Supplementary Figure S4a, short template, and S4b) and found that the FRET ratios for 7–11Cy3 DNAs were essentially identical to those observed for the long template (Supplementary Figure S4c and S4d). The implications of these results are that the polymerase binds to a primer-template junction with an orientation and position that is independent of the sequence context or primer-template length.

KF–DNA binary complex dynamics by smPIFE

In the presence of unlabeled KF, binding and dissociation can also be directly observed by smPIFE of the Cy3 label on the DNA primer-template (19,26). Binding of KF to 6Cy3 DNA results in sudden fluorescence intensity increases (almost double) caused by the change in environment around the fluorophore when KF binds the DNA (Figure 1c and d). These fluctuations are never observed in the absence of KF (Supplementary Figure S3b). Therefore, smPIFE can be used to visualize KF binding and dissociation by normalizing the Cy3 fluorescence intensity to 1.0 in the protein-free state (Figure 1d). It is noteworthy that in the smFRET experiments, we can readily distinguish between FRET and PIFE (Supplementary Figure S5), and therefore, PIFE does not affect our ability to use smFRET to study KF binding.

We determined the fluorescence enhancement for binary complex formation with primer-template junctions from 5–11Cy3 (Figure 2c and e). The observed PIFE remains constant at ~2.1 between 5–8Cy3 and drops abruptly to ~1.2 for 9 and 10Cy3. Beyond 10Cy3 no fluorescence enhancement was observed. These results indicate that the KF footprint on the DNA covers ~8 bp from the primer-template junction, in agreement with previous results (27,28).

Although smPIFE trajectories contain no distance information, they present an advantage over smFRET because Cy5 blinking and photobleaching do not interfere with the PIFE data analysis. Therefore, we used smPIFE to characterize the association and dissociation kinetics of the binary complex. Figure 3a shows representative smPIFE time trajectories with corresponding distributions at [KF] from 0.1 to 5 nM. Dwell time analysis of >100 trajectories at each concentration produces the corresponding pseudo-first order binding (k'_{on}) and dissociation (k_{off}) rate constants (Figure 3b). As expected for a binary reaction the off rate ($k_{off} = 0.37\,s^{-1}$) is concentration independent, while k'_{on} increases linearly with [KF] (Figure 3c). A linear fit to the latter yields the diffusion limited second order dissociation rate constant ($k_{on} = 10^8\,M^{-1}\,s^{-1}$) and the calculated dissociation constant ($K_D = 3.7$ nM) (Figure 3c), comparable to prior results (21,29–31).

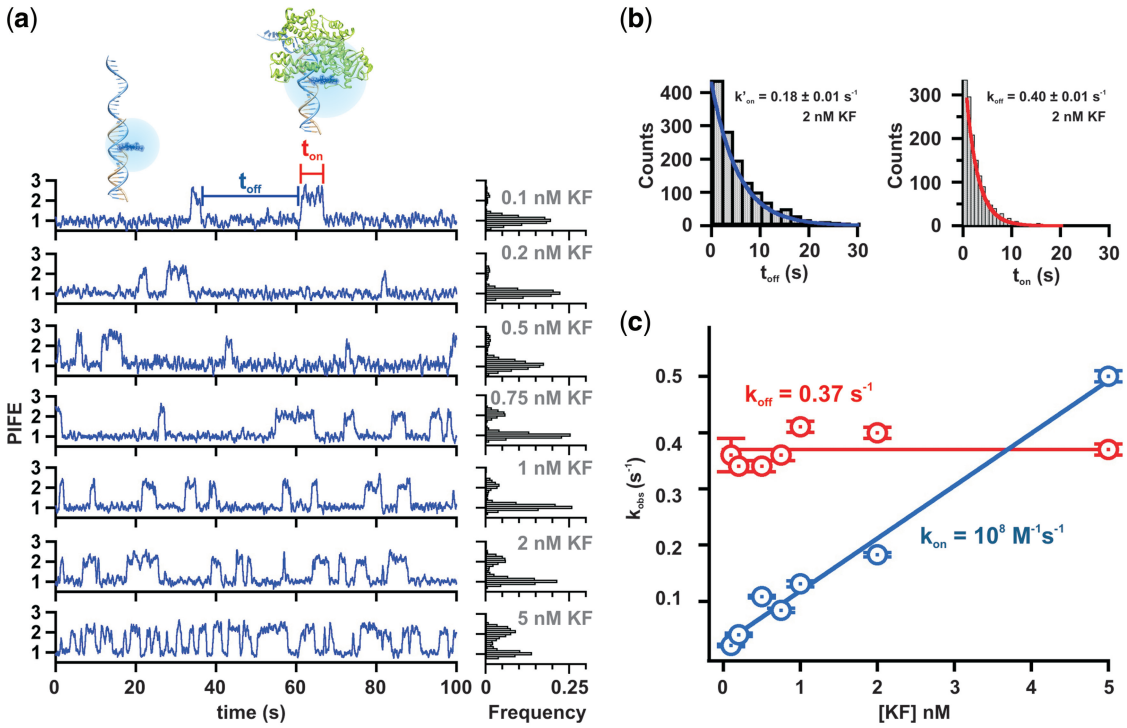

Figure 3. Concentration dependence of KF binding to 8Cy3 observed by smPIFE. (**a**) Representative smPIFE traces and histograms of KF binding to 8Cy3 at increasing concentrations of KF. Unbound DNA has a PIFE value of ~1 until KF binds to the DNA, at which time the PIFE increases to ~2 as shown by the two cartoons. Dwell time analysis was performed to determine the rate of association (k'_{on}) and rate of dissociation (k_{off}) at each KF concentration. (**b**) Representative on and off dwell time distributions and single-exponential fit for 2 nM KF binding to 8Cy3. The on dwell times were determined from the times between binding events (t_{on}) and the off dwell times were measured as the time when KF was bound to the DNA (t_{off}). (**c**) The off (red) and pseudo-first order on (blue) rates as a function of KF concentration. The off rates were independent of KF concentration, while the pseudo-first order on rates had a linear dependence with KF concentration.

Electrostatic competition between KF and NaCl for the DNA

The KF–DNA binary complex is stabilized by electrostatic interactions between the negatively charged phosphate backbone of the DNA and the positively charged basic residues in the polymerase binding cleft (29,32). It is therefore not surprising that ionic strength influences the binary complex stability (33). We used smPIFE to quantify the effect of monovalent ions on KF binding to 8Cy3 DNA in low (0 mM NaCl) and high (100 mM NaCl) salt concetrations. Representative trajectories (Figure 4a) clearly show fewer and shorter-lived binding events in high salt. Dwell time analysis in 0.01–150 mM NaCl (Figure 4b), reveals that salt concentrations >10 mM accelerate KF dissociation (k_{off}) and slow down association (k'_{on}), indicating that salt electrostatically shields the DNA and KF from interacting with each other. One possible interpretation is that high [Na^+] result in both fewer reactive collisions and a less stable binary complex, and thus, slower binding and faster dissociation. We observe a linear relationship between the natural log of the inverse K_D and the natural log of the NaCl concentration (Supplementary Figure S6). The slope of this plot suggests that, under our conditions, one Na^+ ion is released upon binding of the protein to the DNA (34). A previous study suggested that 2.8 K^+ ions may be released upon binding (33). The difference between the two results may be due to the lower overall ionic strength used in the prior study. Finally, at salt concentrations >100 mM, some of the binding events likely become too short to be detected with our time resolution (~50 ms). Nonetheless, our results are consistent with a model where electrostatic interactions between the DNA and KF play an important role in stabilizing the binary complex (29).

NTPs modulate the KF–DNA complex stability

We next used smPIFE to study the effect of correct and incorrect NTPs on the KF binding dynamics. For these experiments, we used a non-extendable 2′,3′-dideoxy terminated primer (8Cy3dd) to prevent nucleotide incorporation. The observed FRET ratio is identical to 8Cy3, indicating that KF binds the dideoxy primer in the same position and orientation as the 3′-OH terminated primer. Dwell time analysis also shows that KF associates with the dideoxy primer with approximately the same rate constant (k'_{on}), although the lack of the 3′-OH did result in a 2-fold decrease in the dissociation rate ($k_{off} = 0.18\ s^{-1}$) (cf. Figure 3 and Supplementary Figure S7). A 2-fold decrease in k_{off} corresponds to ~0.4 kcal/mol stabilization of the binary complex.

In the presence of the next correct nucleotide, in this case dCTP, (Figure 5) numerous binding events longer than 10 min were observed, indicating a more stable

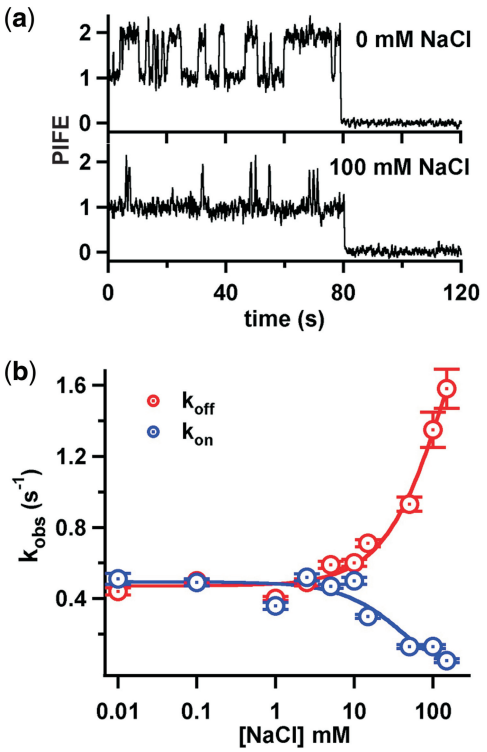

Figure 4. NaCl electrostatically competes with KF for binding to 8Cy3 DNA. (**a**) Comparison of smPIFE trajectories of KF (5 nM) binding to DNA at 0 mM NaCl (top) and 100 mM NaCl (bottom). In both cases, photobleaching of Cy3 occurred at ~80 s. (**b**) Association (blue) and dissociation (red) rates at increasing concentrations of NaCl. The fits are single exponential and the error reported is the error of the single-exponential fits of the dwell times at each NaCl concentration.

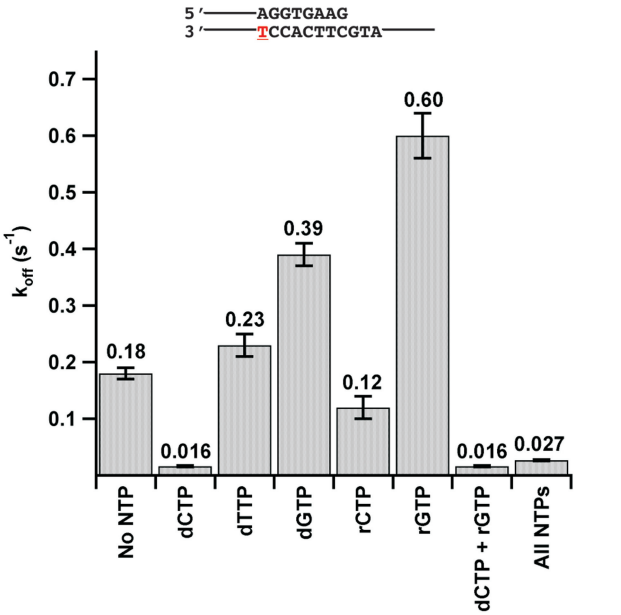

Figure 5. KF rejects incorrect NTPs in favor of the correct dNTP. k_{off} was measured as shown in Figure 3c in the absence or presence of the indicated dNTP or rNTP. Except when all eight NTPs were present, the concentration of nucleotide was 200 μM. When all NTPs were present, the concentration of the dNTPs was 200 μM and the concentration of the rNTPs was 2 mM. All off rates are the averages from titrations of at least five different concentrations of KF (see Supplementary Figure S8), with the exception of the 'dCTP + rGTP' and 'All NTPs' samples in which the off rates were only measured at 0.5 nM KF. The errors are the SDs of the averages, with the exception of the 'dCTP + rGTP' and 'All NTPs' samples in which the errors reported are the errors of the single-exponential fits to the dwell time distributions.

ternary complex. The resulting dissociation rate constant decreases 10-fold ($k_{off} = 0.016\,s^{-1}$), while the association rate remains constant (Supplementary Figure S8). These results show that the correct nucleotide stabilizes the ternary complex by ~1.4 kcal/mol. In the presence of dCTP, the calculated dissociation constant $K_D = 0.16$ nM is in good agreement with prior results (35–37). While this prolonged binding would not be expected to occur during DNA synthesis when the primer contains a 3′-OH, these long binding events suggest the correct nucleotide induces the formation of the stable closed ternary complex that is necessary for phosphodiester bond formation to occur (5).

Similarly, we tested the effect of an incorrect pyrimidine (dTTP) and purine (dGTP). In both cases, the association rate remains constant and only changes in the dissociation constant were observed (Figure 5 and Supplementary Figure S8). Our data reveal that a purine–purine mismatch induces greater destabilization (~0.5 kcal/mol) than a pyrimidine–purine mismatch (~0.1 kcal/mol). Purine–purine mismatches are known to differ significantly from the standard Watson–Crick base pair shape, and therefore, may cause a greater steric clash in the active site during nucleotide selection than pyrimidine–purine mismatches (36,38,39).

In the cell, the concentration of rNTPs is much higher than that of dNTPs (40) and therefore DNA polymerases must also be capable of discriminating between ribo- and deoxynucleotides. In the presence of rGTP, we observe faster dissociation rate constants but similar binding rate constants compared to all other NTPs tested (Figure 5). We find that KF dissociates ~1.5-fold faster in the presence of rGTP compared with dGTP, indicating that the 2′-OH of the incoming nucleotide further destabilizes the ternary complex by ~0.3 kcal/mol. rCTP caused a slightly slower dissociation rate constant compared with no nucleotide, but dissociated ~8-fold faster than in the presence of dCTP (Figure 5 and Supplementary Figure S8). This suggests that rCTP can partially stabilize the ternary complex by ~0.2 kcal/mol. Interestingly, the observed partial stabilization in the presence of rCTP is not a simple compensation between the proper base pairing stabilization (~1.4 kcal/mol) and the 2′-OH destabilization (~0.3 kcal/mol), indicating that additional interactions are involved in the initial discrimination step.

KF readily rejects incorrect NTPs in favor of the correct dNTP

The observed stabilization by the correct dNTP and destabilization by incorrect NTPs, raises the question of how the polymerase selects the correct dNTP in presence of a pool of more highly concentrated incorrect NTPs without the incorrect NTP causing dissociation. To address this question, we measured the association

and dissociation rate constants of KF in presence of an equimolar mixture of dCTP and rGTP, the correct nucleotide and the most destabilizing nucleotide, respectively. Under these conditions we observed an identical dissociation rate constant compared with what was observed for dCTP alone ($k_{off} = 0.016\,s^{-1}$) (Figure 5). When a near-physiological mixture of dNTPs (200 μM) and rNTPs (2 mM) was present, the dissociation rate increased to $0.027\,s^{-1}$. The small change in k_{off} as compared with the presence of only the correct nucleotide is likely due to the increased ionic strength from the counter ions associated with the 8.8 mM nucleotide concentration, which we estimate leads to a ~2-fold rise in k_{off} (Figure 4). Taken together, these results suggest that when a mixture of nucleotides is present the incorrect nucleotide is rejected at a step preceding the proposed steric clash that leads to a faster dissociation rate constant in presence of a single mismatched nucleotide.

Exonuclease site binding only observed with mismatched termini

Structural analysis of KF and its close homologues has shown that the presence of a mismatched primer terminus leads to the movement of the 3′-nucleotide from the polymerase to the exonuclease domain (13,41). Following excision of the mismatched terminal nucleotide, the primer strand presumably reanneals to the template and DNA synthesis resumes. It is interesting, and somewhat surprising, that a crystal structure of KF bound to fully complementary primer-templates shows binding to the exonuclease site (17) and that several ensemble measurements have shown that a fully paired primer binds to the exonuclease site 20–40% of the time (14–16). To test if different smFRET or smPIFE values could be observed for exonuclease site primer binding, we prepared a 9Cy3 primer-template containing two mismatched nucleotides at the primer terminus (Figure 6a). Prior ensemble-averaged studies have shown that such a primer binds exclusively to the exonuclease site (14,18). Our smPIFE data show PIFE values increased from 1.2 for the fully paired primer-template (9Cy3, Figure 2) to 1.8 for the double mismatch (9Cy3mm, Figure 6). Similarly, the smFRET efficiency increased from 0.43 to 0.59. This increase in FRET is consistent with the Cy5 on the polymerase moving closer to the Cy3 on the template and is identical to the value obtained for a fully paired 8Cy3 primer-template (Figures 2 and 6).

Overall, our results indicate that, in the presence of a fully paired primer, the DNA binds exclusively in the polymerase site. In the presence of a mismatched template, the DNA binds in a different orientation consistent with binding in the exonuclease site.

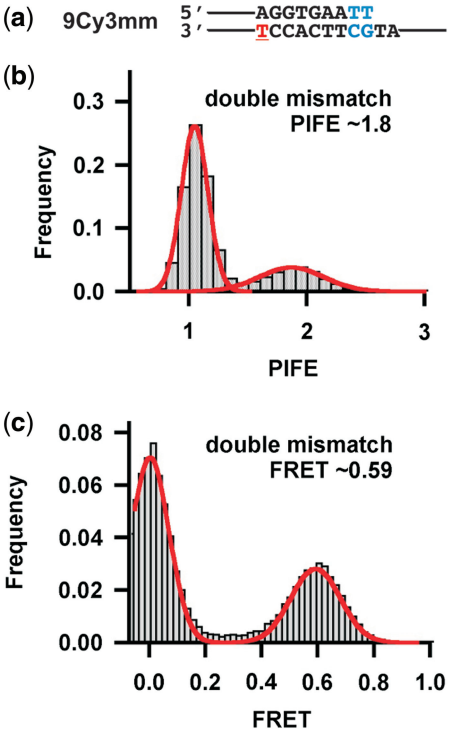

Figure 6. Exonuclease site binding is induced by a double mismatch. (**a**) The double mismatched primer-template structure. (**b**) The PIFE histogram for KF binding to the double mismatched primer-template shown in (a). (**c**) The FRET histogram for KF binding to the double mismatched primer-template shown in (a).

DISCUSSION

We have used smFRET and smPIFE to measure and characterize the binding of KF to DNA primer-templates in real time. KF binding to templates with increasingly longer primers shows that the observed FRET ratios decrease with each addition to the length of the primer, as previously shown (21). Similar experiments measuring smPIFE showed that the PIFE remains unchanged with increasing primer length until the primer-template junction was 9 bp downstream from the Cy3, at which point the PIFE abruptly decreased. As the donor fluorescence enhancement for PIFE requires the interaction between the Cy3 and the DNA polymerase, the sudden decrease in PIFE suggests that the Cy3 is no longer within the footprint region of the polymerase. Our experimentally determined KF footprint of 8 bp is in agreement with previously established ensemble values (27,28).

DNA polymerases must efficiently select against the incorporation of incorrect nucleotides during replication to prevent unacceptably high levels of mutagenesis. For KF, it has been suggested that selection against mispaired rNTPs and dNTPs occurs while the fingers domain is in the open conformation (12,42). Selection against the complementary rNTP is thought to occur as the fingers domain closes (12), at which point the 2′-OH of the ribose sugar has been reported to be sterically blocked by Glu-710 in the polymerase active site (43). In agreement with other ensemble studies (10,36,44), we also find the polymerase–DNA complex was destabilized in the presence of an incorrect dNTP or rNTP, with the notable exception of the rNTP complementary to the templating base, for which we observed stabilized polymerase binding. Another single-molecule study suggested the fingers domain of the polymerase was in a 'partially closed' state in the presence of the complementary

rNTP, which also could lead to increased stability of the polymerase–DNA–complementary rNTP complex (6).

The destabilizing effect of mismatched nucleotides is difficult to square with the requirement for a DNA polymerase to remain bound to the DNA template during processive DNA synthesis. While it is easy to understand how the next correct dNTP causes an enhanced stability of the polymerase–DNA complex by triggering a conformational change from the open binary to the more stable closed ternary complex, the destabilizing effect of non-complementary dNTPs and rNTPs, which are present in large excess over the properly paired dNTP (40), is counterintuitive, especially considering the evidence that most mispaired nucleotides seem to be rejected prior to the closing of the fingers (12). However, when we measured the dissociation rates for KF in the presence of mixtures of correct and incorrect nucleotides, even where the incorrect nucleotides are present in large excess, we found that the k_{off} remains essentially unchanged compared with that observed when only the correct nucleotide is present.

We conclude from these results that there appears to be a different mechanism in place when only an incorrect nucleotide is present compared with a mixture of correct and incorrect. Although we cannot be sure of the mechanism causing these effects without further structural characterization of the polymerase complex in the presence of an incorrect nucleotide, one possible explanation for this observation that is consistent with the prior studies (12,42) is that the presence of only the incorrect nucleotide allows the movement of the templating base from the pre-insertion to insertion site, possibly at a much slower rate compared with a correct nucleotide. In this scenario, when a mixture of nucleotides is present, incorrect nucleotides are rejected at the pre-insertion site until a correct nucleotide binds. However, in the absence of the correct nucleotide, eventually a mispaired nucleotide results in the movement of the nascent base pair to the insertion site, causing the initiation of fingers closure and a steric clash in the active site induced by the mispair and resulting in an enhanced dissociation rate of the polymerase. In addition, the dissociation rate constants and K_Ds in the presence of different mispairing dNTPs (10) show that the larger the size of the mispair the less stable the binding of KF to the primer-template. Thus, it appears that the larger the size of the mispair, the greater the steric clash when the fingers closure initiates.

Under the rare circumstances that misincorporation of a non-complementary nucleotide occurs, there is substantial evidence that several terminal base pairs melt and the single-stranded primer DNA is transferred to the exonuclease site (13,17). This placement allows for the excision of the incorrect terminal 3′-nucleotide followed by the return of the primer strand to the polymerase site for continued synthesis. KF binding at the exonuclease site is thought to cause the movement of the polymerase upstream along the duplex DNA by ~2 or 3 nt (45).

Crystallographic and several ensemble biochemical studies have suggested that even when the primer-template is properly paired, the primer strand can show significant levels of partitioning to the exonuclease site (14,15,17). Here, we have shown that we can use both smFRET and smPIFE to detect exonuclease site binding using a double mismatched primer-template, which has been shown to bind exclusively to the exonuclease site (14,18). Using these techniques, we have attempted to detect either exonuclease site binding for a paired primer-template or dynamic exchange between exonuclease and polymerase site binding. In our hands, we see no evidence that a properly paired template is positioned outside of the polymerase active site. This raises the question of what factors might lead to the differences observed for the ensemble studies and these single-molecule results.

When the crystal structure of KF was first published, it was surprising that it showed the primer terminus bound exclusively to the exonuclease site (17). However, the co-crystals of the DNA and KF were formed at high ionic strength and it is possible these conditions reduced the frequency of polymerase site binding. Fluorescence depolarization studies were later used to measure the partition coefficient for movement between the polymerase site and exonuclease site and found that up to 14% of the primer termini were in the exonuclease site, depending on the sequence at the 3-terminus of the primer (14). Fluorescence and circular dichroism measurements of primers containing 2-aminopurines as the two 3′-terminal base pairs showed about a 43% occupancy in the exonuclease site (15). However, these studies were performed in the presence of Ca^{2+} rather than Mg^{2+} and it is unclear if the 2-aminopurine contributed to higher levels of exonuclease binding. Finally, surface plasmon resonance has been used to measure the dissociation rates from DNA bound to the polymerase site and exonuclease site (18). Similar to our work, these studies were carried out with DNA containing no modifications near the primer-template junction and under standard polymerase buffer conditions and showed that ~97% of the polymerase molecules had the primer bound in the polymerase site.

The work herein provides a comprehensive assessment of DNA polymerase binding dynamics with DNA at the single-molecule level. We have utilized two distinct approaches, smFRET and smPIFE, to observe the interactions between the polymerase and the DNA in real time. We found these two approaches naturally complement each other by individually providing unique information about the system. smFRET enables us to track the position of the polymerase on the DNA with single-base pair resolution and can be used to distinguish between polymerase and exonuclease site binding. smPIFE, which is not affected by acceptor bleaching or blinking, was used to determine the binding kinetics in absence and presence of dNTPs and rNTPs, and was able to precisely measure the binding footprint of KF on DNA. In the future, this method can easily be used to study other DNA binding proteins, to characterize the potentially mutagenic interactions of DNA polymerases with mispaired primer termini or carcinogenic adducts linked to the DNA and to investigate further the mechanism by which DNA polymerases maintain their remarkable fidelity.

SUPPLEMENTARY DATA

Supplementary Data are available at NAR Online: Supplementary Table 1 and Supplementary Figures 1–8.

ACKNOWLEDGEMENTS

R.M., K.V., L.R. and D.R. designed the experiments. R.M. and K.V. carried out the experiments. R.M., K.V., L.R. and D.R. wrote the manuscript.

FUNDING

National Institutes of Health (NIH) [CA40605 to L.J.R., GM085116 to D.R.]; National Science Foundation CAREER Award [MCB0747285 to D.R.]. Funding for open access charge: NIH.

Conflict of interest statement. None declared.

REFERENCES

1. Kornberg,A., Lehman,I.R. and Simms,E.S. (1956) Polydesoxyribonucleotide synthesis by enzymes from Escherichia coli. *Fed. Proc*, **15**, 291–292.
2. Brutlag,D., Atkinson,M.R., Setlow,P. and Kornberg,A. (1969) An active fragment of DNA polymerase produced by proteolytic cleavage. *Biochem. Biophys. Res. Commun.*, **37**, 982–989.
3. Klenow,H. and Henningsen,I. (1970) Selective elimination of the exonuclease activity of the deoxyribonucleic acid polymerase from Escherichia coli B by limited proteolysis. *Proc. Natl Acad. Sci. USA*, **65**, 168–175.
4. Steitz,T.A. (1999) DNA polymerases: structural diversity and common mechanisms. *J. Biol. Chem.*, **274**, 17395–17398.
5. Doublie,S., Sawaya,M.R. and Ellenberger,T. (1999) An open and closed case for all polymerases. *Structure*, **7**, R31–R35.
6. Santoso,Y., Joyce,C.M., Potapova,O., Le Reste,L., Hohlbein,J., Torella,J.P., Grindley,N.D. and Kapanidis,A.N. (2010) Conformational transitions in DNA polymerase I revealed by single-molecule FRET. *Proc. Natl Acad. Sci. USA*, **107**, 715–720.
7. Astatke,M., Grindley,N.D. and Joyce,C.M. (1995) Deoxynucleoside triphosphate and pyrophosphate binding sites in the catalytically competent ternary complex for the polymerase reaction catalyzed by DNA polymerase I (Klenow fragment). *J. Biol. Chem.*, **270**, 1945–1954.
8. Doublie,S., Tabor,S., Long,A.M., Richardson,C.C. and Ellenberger,T. (1998) Crystal structure of a bacteriophage T7 DNA replication complex at 2.2 A resolution. *Nature*, **391**, 251–258.
9. Li,Y., Korolev,S. and Waksman,G. (1998) Crystal structures of open and closed forms of binary and ternary complexes of the large fragment of Thermus aquaticus DNA polymerase I: structural basis for nucleotide incorporation. *EMBO J.*, **17**, 7514–7525.
10. Dzantiev,L. and Romano,L.J. (2000) A conformational change in E. coli DNA polymerase I (Klenow fragment) is induced in the presence of a dNTP complementary to the template base in the active site. *Biochemistry*, **39**, 356–361.
11. Johnson,S.J., Taylor,J.S. and Beese,L.S. (2003) Processive DNA synthesis observed in a polymerase crystal suggests a mechanism for the prevention of frameshift mutations. *Proc. Natl Acad. Sci. USA*, **100**, 3895–3900.
12. Joyce,C.M., Potapova,O., Delucia,A.M., Huang,X., Basu,V.P. and Grindley,N.D. (2008) Fingers-closing and other rapid conformational changes in DNA polymerase I (Klenow fragment) and their role in nucleotide selectivity. *Biochemistry*, **47**, 6103–6116.
13. Beese,L.S., Derbyshire,V. and Steitz,T.A. (1993) Structure of DNA polymerase I Klenow fragment bound to duplex DNA. *Science*, **260**, 352–355.
14. Carver,T.E. Jr, Hochstrasser,R.A. and Millar,D.P. (1994) Proofreading DNA: recognition of aberrant DNA termini by the Klenow fragment of DNA polymerase I. *Proc. Natl Acad. Sci. USA*, **91**, 10670–10674.
15. Datta,K., Johnson,N.P., Licata,V.J. and von Hippel,P.H. (2009) Local conformations and competitive binding affinities of single- and double-stranded primer-template DNA at the polymerization and editing active sites of DNA polymerases. *J. Biol. Chem.*, **284**, 17180–17193.
16. Datta,K., Johnson,N.P. and von Hippel,P.H. (2010) DNA conformational changes at the primer-template junction regulate the fidelity of replication by DNA polymerase. *Proc. Natl Acad. Sci. USA*, **107**, 17980–17985.
17. Freemont,P.S., Friedman,J.M., Beese,L.S., Sanderson,M.R. and Steitz,T.A. (1988) Cocrystal structure of an editing complex of Klenow fragment with DNA. *Proc. Natl Acad. Sci. USA*, **85**, 8924–8928.
18. Tsoi,P.Y., Zhang,X., Sui,S.F. and Yang,M. (2003) Effects of DNA mismatches on binding affinity and kinetics of polymerase-DNA complexes as revealed by surface plasmon resonance biosensor. *Analyst*, **128**, 1169–1174.
19. Hwang,H., Kim,H. and Myong,S. (2011) Protein induced fluorescence enhancement as a single molecule assay with short distance sensitivity. *Proc. Natl Acad. Sci. USA*, **108**, 7414–7418.
20. Joyce,C.M. and Derbyshire,V. (1995) Purification of Escherichia coli DNA polymerase I and Klenow fragment. *Methods Enzymol.*, **262**, 3–13.
21. Christian,T.D., Romano,L.J. and Rueda,D. (2009) Single-molecule measurements of synthesis by DNA polymerase with base-pair resolution. *Proc. Natl Acad. Sci. USA*, **106**, 21109–21114.
22. Lamichhane,R., Solem,A., Black,W. and Rueda,D. (2010) Single-molecule FRET of protein-nucleic acid and protein-protein complexes: surface passivation and immobilization. *Methods*, **52**, 192–200.
23. Zhao,R. and Rueda,D. (2009) RNA folding dynamics by single-molecule fluorescence resonance energy transfer. *Methods*, **49**, 112–117.
24. Guo,Z., Karunatilaka,K.S. and Rueda,D. (2009) Single-molecule analysis of protein-free U2-U6 snRNAs. *Nat. Struct. Mol. Biol.*, **16**, 1154–1159.
25. Karunatilaka,K.S., Solem,A., Pyle,A.M. and Rueda,D. (2010) Single-molecule analysis of Mss116-mediated group II intron folding. *Nature*, **467**, 935–939.
26. Luo,G., Wang,M., Konigsberg,W.H. and Xie,X.S. (2007) Single-molecule and ensemble fluorescence assays for a functionally important conformational change in T7 DNA polymerase. *Proc. Natl Acad. Sci. USA*, **104**, 12610–12615.
27. Joyce,C.M. and Steitz,T.A. (1987) DNA-polymerase-i - from crystal-structure to function via genetics. *Trends Biochem. Sci.*, **12**, 288–292.
28. Allen,D.J., Darke,P.L. and Benkovic,S.J. (1989) Fluorescent oligonucleotides and deoxynucleotide triphosphates: preparation and their interaction with the large (Klenow) fragment of Escherichia coli DNA polymerase I. *Biochemistry*, **28**, 4601–4607.
29. Halford,S.E. (2009) An end to 40 years of mistakes in DNA-protein association kinetics? *Biochem. Soc. Trans.*, **37**, 343–348.
30. Kuchta,R.D., Mizrahi,V., Benkovic,P.A., Johnson,K.A. and Benkovic,S.J. (1987) Kinetic mechanism of DNA polymerase I (Klenow). *Biochemistry*, **26**, 8410–8417.
31. Polesky,A.H., Steitz,T.A., Grindley,N.D. and Joyce,C.M. (1990) Identification of residues critical for the polymerase activity of the Klenow fragment of DNA polymerase I from Escherichia coli. *J. Biol. Chem.*, **265**, 14579–14591.
32. Warwicker,J., Ollis,D., Richards,F.M. and Steitz,T.A. (1985) Electrostatic field of the large fragment of Escherichia coli DNA polymerase I. *J. Mol. Biol.*, **186**, 645–649.
33. Datta,K. and LiCata,V.J. (2003) Salt dependence of DNA binding by Thermus aquaticus and Escherichia coli DNA polymerases. *J. Biol. Chem.*, **278**, 5694–5701.
34. Lohman,T.M. and Mascotti,D.P. (1992) Thermodynamics of ligand-nucleic acid interactions. *Methods Enzymol.*, **212**, 400–424.

35. Dzantiev,L. and Romano,L.J. (1999) Interaction of Escherichia coli DNA polymerase I (Klenow fragment) with primer-templates containing N-acetyl-2-aminofluorene or N-2-aminofluorene adducts in the active site. *J. Biol. Chem.*, **274**, 3279–3284.
36. Dzantiev,L., Alekseyev,Y.O., Morales,J.C., Kool,E.T. and Romano,L.J. (2001) Significance of nucleobase shape complementarity and hydrogen bonding in the formation and stability of the closed polymerase-DNA complex. *Biochemistry*, **40**, 3215–3221.
37. Lone,S. and Romano,L.J. (2003) Mechanistic insights into replication across from bulky DNA adducts: a mutant polymerase I allows an N-acetyl-2-aminofluorene adduct to be accommodated during DNA synthesis. *Biochemistry*, **42**, 3826–3834.
38. Kool,E.T., Morales,J.C. and Guckian,K.M. (2000) Mimicking the structure and function of DNA: insights into DNA stability and replication. *Angew. Chem. Int. Ed. Engl*, **39**, 990–1009.
39. Trostler,M., Delier,A., Beckman,J., Urban,M., Patro,J.N., Spratt,T.E., Beese,L.S. and Kuchta,R.D. (2009) Discrimination between right and wrong purine dNTPs by DNA polymerase I from Bacillus stearothermophilus. *Biochemistry*, **48**, 4633–4641.
40. Mathews,C.K. (1972) Biochemistry of deoxyribonucleic acid-defective amber mutants of bacteriophage T4. 3. Nucleotide pools. *J. Biol. Chem.*, **247**, 7430–7438.
41. Ollis,D.L., Brick,P., Hamlin,R., Xuong,N.G. and Steitz,T.A. (1985) Structure of large fragment of Escherichia coli DNA polymerase I complexed with dTMP. *Nature*, **313**, 762–766.
42. Rothwell,P.J. and Waksman,G. (2007) A pre-equilibrium before nucleotide binding limits fingers subdomain closure by Klentaq1. *J. Biol. Chem.*, **282**, 28884–28892.
43. Astatke,M., Ng,K., Grindley,N.D. and Joyce,C.M. (1998) A single side chain prevents Escherichia coli DNA polymerase I (Klenow fragment) from incorporating ribonucleotides. *Proc. Natl Acad. Sci. USA*, **95**, 3402–3407.
44. Garalde,D.R., Simon,C.A., Dahl,J.M., Wang,H., Akeson,M. and Lieberman,K.R. (2011) Distinct complexes of DNA polymerase I (Klenow fragment) for base and sugar discrimination during nucleotide substrate selection. *J. Biol. Chem.*, **286**, 14480–14492.
45. Joyce,C.M. and Steitz,T.A. (1994) Function and structure relationships in DNA polymerases. *Annu. Rev. Biochem.*, **63**, 777–822.